



An investigation of fatigue damage development under complete contact fretting test conditions

Citation

Holopainen, S., Juoksukangas, J., Kouhia, R., Lehtovaara, A., & Saksala, T. (2016). An investigation of fatigue damage development under complete contact fretting test conditions. *Rakenteiden mekaniikka*, 49(3), 151-159.

Year

2016

Version

Publisher's PDF (version of record)

Link to publication

[TUTCRIS Portal \(http://www.tut.fi/tutcris\)](http://www.tut.fi/tutcris)

Published in

Rakenteiden mekaniikka

Copyright

This is an open access article licensed under the Creative Commons Attribution-ShareAlike 4.0 International license. To view a copy of this license, visit <http://creativecommons.org/licenses/by-sa/4.0/>

Take down policy

If you believe that this document breaches copyright, please contact cris.tau@tuni.fi, and we will remove access to the work immediately and investigate your claim.

An investigation of fatigue damage development under complete contact fretting test conditions

Sami Holopainen, Janne Juoksukangas, Reijo Kouhia¹, Arto Lehtovaara, Timo Saksala

Summary. In this paper evolution equation based multiaxial fatigue model is applied to the analysis of fretting fatigue of a cantilever test specimen made of EN 10083-1 steel. The adopted high-cycle fatigue model is based on the concept of evolving endurance surface and damage evolution equation. For the endurance surface a simple linear relationship between the hydrostatic stress and the reduced deviatoric stress is used. It is observed that such a simple relationship does not model the fretting fatigue phenomena properly due to the high compressive hydrostatic stress state at the contact region. Also stress gradient effects should be taken into account in a more rigorous manner.

Key words: fretting fatigue, high-cycle fatigue model, endurance surface

Received 11 November 2016. Accepted 28 December 2016. Published online 30 December 2016.

Introduction

Design against fatigue constitutes an integral part of mechanical engineering analysis. The design can benefit from capable models and the strong computational capability available nowadays. To evaluate models, reliable testing for long-term service life is mandatory. The paper focuses on the investigation of fatigue damage development on metals under accelerated, complete contact fretting test conditions. The model applied to the evaluation is proposed by Ottosen, Stenström and Ristinmaa in 2008 [11], which model is formulated in a rate form within continuum mechanics framework without the need to measure damage changes per loading cycles. The model is implemented in a finite-element program and the role of the test conditions on the fretting fatigue is discussed.

Fretting refers to a small amplitude tangential movement between two contacting bodies. Even a small oscillating micrometer level movement can cause wear of the contacting bodies and significant decrease in fatigue life due to high stresses induced by the frictional movement [1, 4]. The stress state in fretting contacts is typically multiaxial and non-proportional. Fretting creates steep stress gradients and typically some averaging of stresses is needed to match the predicted fretting fatigue life with experiments. The theory of critical distances [14] can be used for such a purpose, for example. It is important to predict fretting fatigue life. Different kinds of fatigue methodologies have been applied to fretting using for example, multiaxial fatigue models, such as critical plane methods

¹Corresponding author. reijo.kouhia@tut.fi

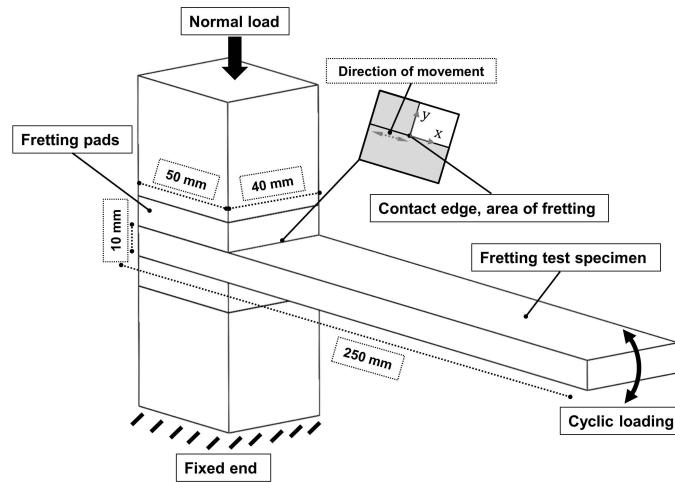


Figure 1. Testing arrangement [5].

[9], equivalent stress methods such as von Mises [8] and fracture mechanics [10] to study fretting cracking, lifetime and cracking point. In addition, fretting-parameters have been developed, such as the Ruiz criterion [13]. However, these criteria are static and in principle cannot be used for arbitrary loading conditions. In this paper an evolution equation based multiaxial high-cycle fatigue model is applied to the fretting fatigue problem for the first time.

In fretting fatigue there are certain common characteristics to the cracks generated by a wide range of fretting geometries: (i) the cracks nucleate at the edge of the contact or a fretting induced stress concentration inside the contact and (ii) the early crack growth is in mode II loading. Due to that, the cracks beneath the contact area propagate first at some oblique angle - typically in the direction of 45 degrees to the surface [7, 15]. At some length the crack turns to an orientation corresponding to the maximum mode I stress intensity.

Fretting tests and corresponding model

The test specimen is made of the 34CrNiMo6 steel (EN-10083-1+QT) and has dimensions 250 mm x 40 mm x 10 mm. Dimensions of the contact area are 50 mm x 40 mm. The test device and procedure are described in detail in [5]. A view of the device is shown in Fig. 1. The test specimen is clamped between two flat-ended pads and a normal load is applied by a hydraulic actuator which guarantees that no tangential loads are produced during the application of normal load. The normal load can be adjusted continuously resulting up to an average contact pressure of 300 MPa. For the fatigue testing cyclic load is generated at the free end of the specimen by an eccentric mechanism and the driving frequency 41 Hz was used.

The used finite element model includes the fretting specimen, pads and two blocks of steel as shown in Fig 1. The two contacts are modelled between the specimen and pads but the pads and blocks of steel are adhered to each other. The bottom end of the lower block shown in Fig 1 is fixed in y -direction. The center of the lowest and uppermost edges (of the corresponding blocks of steel) is fixed in x -direction, i.e., in the direction of fretting movement. The normal pressure is applied on the top of the upper block and cyclic transverse loading (displacement) at the tip of the cantilever specimen. An implicit

finite element analysis was carried out. The used element type was CPE4I and the size of the smallest element at the contact edge was 5 μm .

According to a convergence analysis the maximum difference between the results of a model having half-sized elements (2.5 μm) and the present model is below 2.3 % for the von Mises stress value at the chosen point of inspection.² The fatigue model is implemented in the commercial FE-solver Abaqus as a user subroutine. After a stabilized cycle period the stress state at the chosen point is used in a post-processing routine which is used to compute the fatigue life.

High-cycle fatigue model

Ottosen, Stenström and Ristinmaa proposed in 2008 an evolution equation based high-cycle fatigue model which is based on a concept of an evolving endurance surface and damage variable [11]. Such an approach treats multiaxial stress states and arbitrary loading sequences in a unified manner and the cycle-counting techniques are not needed.

For isotropic high-cycle fatigue the endurance surface proposed in [11] has the following form

$$\beta = \frac{1}{\sigma_{-1}}(\bar{\sigma} + AI_1 - \sigma_{-1}) = 0, \quad (1)$$

where I_1 is the first invariant of the stress tensor $\boldsymbol{\sigma}$, i.e. $I_1 = \text{tr } \boldsymbol{\sigma}$, and the effective stress $\bar{\sigma}$ is defined by the second invariant of the reduced deviatoric stress $\mathbf{s} - \boldsymbol{\alpha}$ as

$$\bar{\sigma} = \sqrt{3J_2(\mathbf{s} - \boldsymbol{\alpha})} = \sqrt{\frac{3}{2} \text{tr}(\mathbf{s} - \boldsymbol{\alpha})^2}. \quad (2)$$

The deviatoric stress tensor is $\mathbf{s} = \boldsymbol{\sigma} - \frac{1}{3} \text{tr}(\boldsymbol{\sigma})\mathbf{I}$, where \mathbf{I} stands for the identity tensor. The endurance limit at zero mean stress is denoted as σ_{-1} . The non-dimensional positive parameter A is the opposite value of the slope in the Haigh diagram and can be determined e.g. using formula $A = (\sigma_{-1}/\sigma_0) - 1$, where σ_0 is the fatigue limit amplitude for tensile pulsating loading. A back stress like deviatoric tensor $\boldsymbol{\alpha}$ is a history variable. It is responsible for the movement of the endurance surface (1) in the stress space. Evolution of the $\boldsymbol{\alpha}$ -tensor is governed by the evolution equation

$$\dot{\boldsymbol{\alpha}} = C(\mathbf{s} - \boldsymbol{\alpha})\dot{\beta}, \quad (3)$$

where C is a positive dimensionless material parameter and the superimposed dot denotes time rate. Shape of the endurance surface in the deviatoric plane is circular and the meridian lines are straight as with the case of the Drucker-Prager model in plasticity, see Figs. 2 and 3.

Despite damage resulting principally from the initiation, nucleation, and growth of voids and micro-cracks generate anisotropic behaviour, material damage is modelled macroscopically using an isotropic damage variable $D \in [0, 1]$, for which the evolution is governed by the equation of the form

$$\dot{D} = \frac{K}{(1 - D)^k} \exp(L\beta)\dot{\beta} \quad (4)$$

where $K > 0$, $L > 0$ and $k \geq 0$ are material parameters. Since $\dot{D} \geq 0$ and damage never decreases, it then follows that for damage evolution $\dot{\beta} \geq 0$. In contrast to plasticity, the

²With the highest bulk loading and using the value of 0.6 for the coefficient of friction.

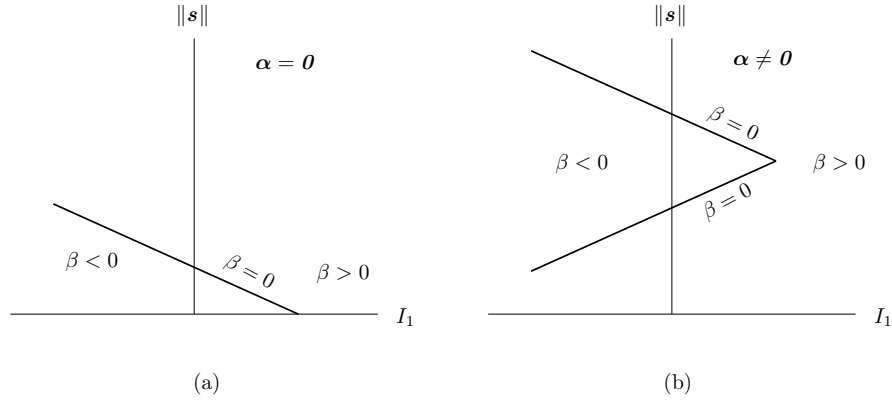


Figure 2. Endurance surface presented in a meridian plane as the backstress is (a) $\alpha = 0$ and (b) $\alpha \neq 0$.

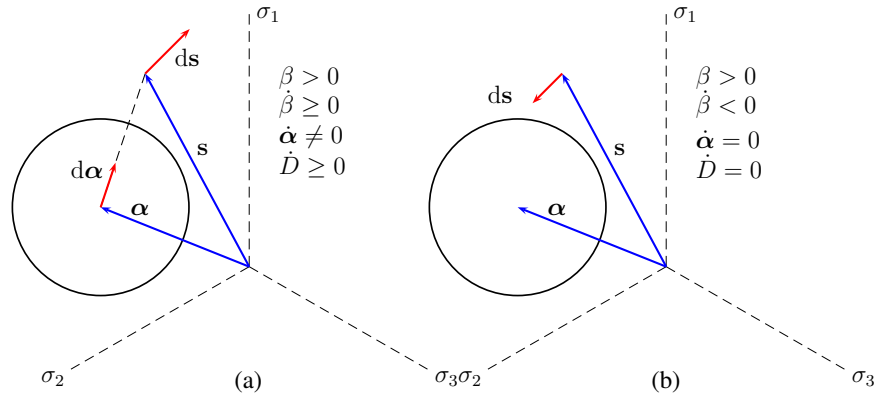


Figure 3. (a) Movement of the endurance surface and damage growth when the stress is outside the endurance surface and moving away from it. (b) When the stress is outside the endurance surface but the stress increment is directed towards the endurance surface, damage and back stress does not evolve.

stress state can lie outside the endurance surface. When the stress state is outside the endurance surface and moves away from this surface, i.e. the evolution of the α -tensor and damage takes place when

$$\beta \geq 0 \quad \text{and} \quad \dot{\beta} > 0, \quad (5)$$

see Fig. 3.

In this paper the value $k = 0$, as in [11], has been used. It means that in a constant amplitude cyclic loading the damage increase per cycle will saturate to a constant value. However, in reality the damage rate increases with increasing damage and an alternative formulation with $k = 1$ is used in [3]. In that case, i.e. $k \geq 0$, damage rate per cycle increases with increasing damage, see the results in [2, Figures 6 and 7].

Fatigue model calibration

The model contains only the parameters σ_{-1} , A , C , K , and L , which are calibrated from experimental data.

The concept for the calibration of the remaining parameters C , K , and L is analogous to that given in [11, Section 5]. According to this concept, the evolution equations for the

Table 1. Estimated material parameters for the 34CrNiMo6 steel.

σ_{-1} [MPa]	A when $I_1 > 0$	A when $I_1 < 0$	C	K	L
501	0.285	0.06	0.5	$9.0 \cdot 10^{-5}$	6.38

backstress and damage are first integrated in order to define the damage accumulation per a loading cycle and the number of cycles N needed to fatigue failure. The expression of n is then employed as a single constraint function in the least squares fitting which is based on the Nelder-Mead simplex algorithm. The least squares error of number of cycles N which leads to fatigue failure is chosen as the object function f to be minimized, i.e.

$$f = \sum_{i=1}^m (w^{(i)})^2 \left(1 - \frac{\ln(N^{(i)})}{\ln(N_{em}^{(i)})} \right)^2 \quad (6)$$

where m is the number of experimental points, $w^{(i)}$ are the weights, and $N^{(i)}$ and $N_{em}^{(i)}$ denote the number of cycles predicted by the model and recorded in the experiments, respectively.

The parameters C , K and L have been determined based on the base material S-N curve ($R = -1$) given in [12, Chapter 18.1] is

$$\sigma_a = \frac{\sigma^*}{(N/N^*)^{1/n}} \quad (7)$$

where $N^* = 6.3 \cdot 10^5$, $\sigma^* = 462$ MPa and $n = 11.6$.

Model results and discussion

The model described above has been implemented into the commercial finite element code Abaqus using the user material subroutine. Also a post-processing subroutine is written, which can be used for the fatigue life prediction after a stable stress cycle is reached.

The experimental fretting fatigue data originally presented in [5] and a similar kind of finite element model as presented in [6] was utilized in this study. Finer mesh and the coefficient of friction 0.6 was used here. A cracked surface of a test specimen is shown in Fig. 4. The model predicts that fatigue damage nucleates at the contact edge and propagates approximately normal to the contact surface, see Fig. 5. The results match qualitatively with the experimental observations, performed by eye inspection. In the real fretting specimens, cracks have nucleated in the central region of the contact edge in the lateral direction. No cracks clearly nucleated from the corners while several initial cracks typically nucleated along the contact edge once they coalesced into larger cracks during loading.

The results of both the model and test series are presented here in the form of S- N curves in Fig. 6. Stresses beneath the contact surface were extracted at the chosen distance of $12.5 \mu\text{m}$. The point under inspection is shown in Fig. 5. The measured maximum bending stress amplitude in the specimen is plotted against the number of cycles required for macroscopic crack initiation in a case where the average contact pressure is 100 MPa. The damage model predicts whether a crack is formed or not and therefore, to accurately determine the total fretting fatigue life, crack propagation should be taken into account.

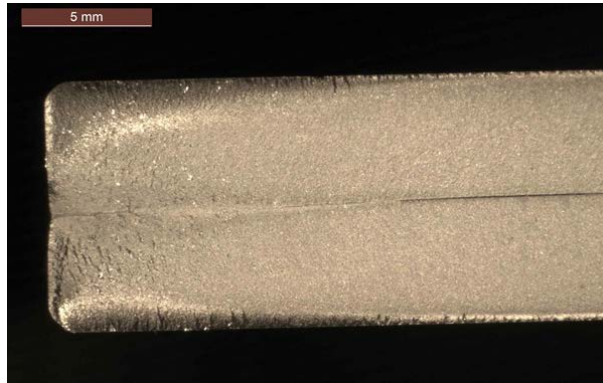


Figure 4. Cracked surface of the fretting specimen.

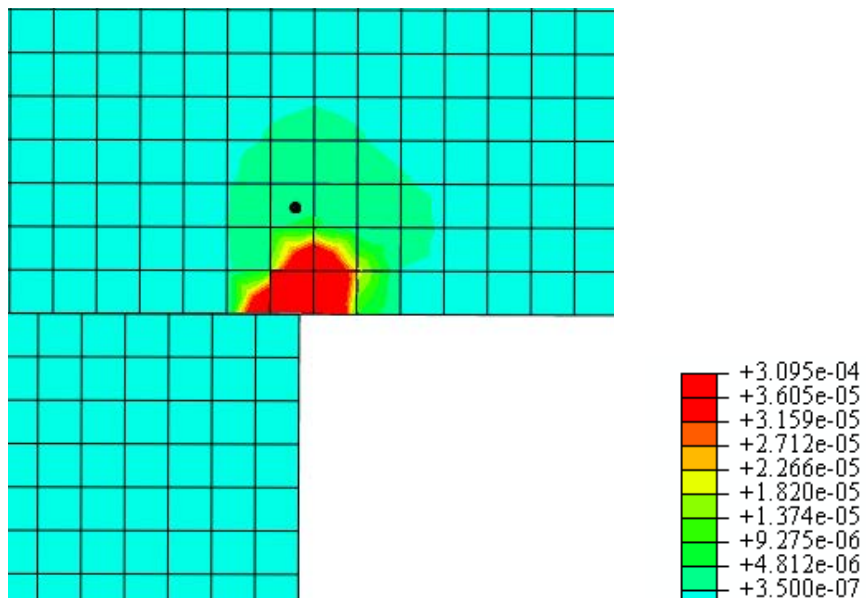


Figure 5. Damage field in the numerical model after 16 cycles at the contact corner point. Maximum value of damage is $3.1 \cdot 10^{-4}$. The size of the smallest element is $5 \mu\text{m}$.

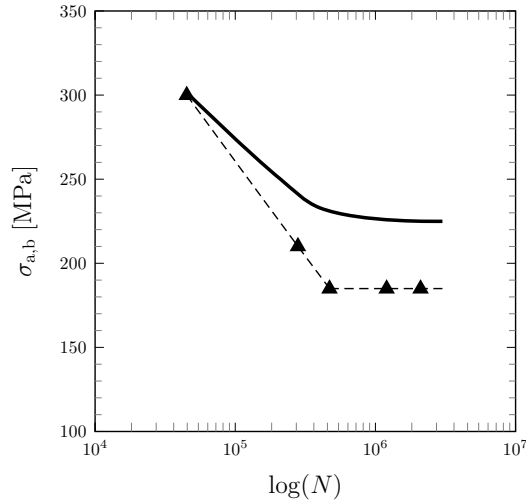


Figure 6. Fatigue strengths of the 34CrNiMo6 steel. The solid line is the model response and the markers denote the experimental data from [5]. N is the number of cycles required for macroscopic crack initiation.

The crack nucleation time is difficult to determine experimentally. However, fatigue limits may be compared approximately.

The points at over three million cycles are run-outs, where the specimens have not been cracked. The lifetime decreases as the bending stress amplitude increases. The fretting fatigue limit obtained from the tests is about 170 MPa, which is only one-third of the plain fatigue limit of the material.

The evolution equation based fatigue model used in this study overestimates clearly the fatigue limit, see Fig. 6. This is mainly due to the inability of the linear relationship between the effective stress and the hydrostatic stress in the expression of the endurance surface to model cases where there exist high compressive stresses. In obtaining the model results shown in Fig. 6, the A -parameter has the value 0.06 when the invariant I_1 is negative. However, this simple correction is not enough to capture the true fatigue behaviour observed from this fretting experiment. Therefore, a more precise form of the endurance surface is needed to capture the whole allowable stress range in the Haigh-representation. The FE-model input values such as coefficient of friction and the sub-surface distance chosen have an effect on stress state, which may partly explain the difference, but this was not studied in detail.

Concluding remarks

It is observed that in analysing fretting fatigue with the evolution equation based fatigue model proposed by Ottosen et al. [11], the simple linear relation between the effective stress and the first invariant of the stress tensor is not sufficiently accurate. This is due to the high pressure at the contact area which results in negative values of the hydrostatic stress. Possible remedies could be the reformulation of the endurance surface and/or to replace the first invariant with the maximum principal stress. The FE-model input values may also partly explain the difference between numerical and experimental results. Also the selected distance from the contact surface as a basis of the cyclic stress state has a big influence on the results. Applying gradient type models would be an alternative approach to take steep gradients into account in a more rigorous manner.

Acknowledgements

This work has been supported in part by Tekes - the National Technology Agency of Finland, project SCarFace, decision number 40205/12. The tests have been done within the DEMAPP program financed by FIMECC Ltd.

References

- [1] D.A. Hills and D. Nowell. *Mechanics of Fretting Fatigue*. Kluwer Academic Publishers, Dordrecht, 1994.
- [2] S. Holopainen, R. Kouhia, J. Könnö, and T. Saksala. Computational modelling of transversely isotropic high-cycle fatigue using a continuum based model. *Procedia Structural Integrity*, 2:2718–2725, 2016.
- [3] S. Holopainen, R. Kouhia, and T. Saksala. Continuum approach for modeling transversely isotropic high-cycle fatigue. *European Journal of Mechanics A/Solids*, 60: 183–195, 2016.
- [4] K.L. Johnson. *Contact Mechanics*. Cambridge University Press, Cambridge, UK, 1985.
- [5] J. Juoksukangas, A. Lehtovaara, and A. Mäntylä. Development of a complete contact fretting test device. *Journal of Engineering Tribology*, 227:570–578, 2012.
- [6] J. Juoksukangas, A. Lehtovaara, and A. Mäntylä. A comparison of relative displacement fields between numerical predictions and experimental results in fretting contact. *Journal of Engineering Tribology*, 230(10):1273–1287, 2016. doi:[10.1016/1350650116633572](https://doi.org/10.1016/1350650116633572).
- [7] H. Lee, O. Jin, and S. Mall. Fretting fatigue behavior of Ti-6Al-4V with dissimilar mating materials. *International Journal of Fatigue*, 26:393–402, 2004. doi:[10.1061/j.ijfatigue.2003.07.004](https://doi.org/10.1061/j.ijfatigue.2003.07.004).
- [8] S.B. Leen, I.R. McColl, C.H.H. Ratsimba, and E.J. Williams. Fatigue life prediction for a barrelled spline coupling under torque overload. *Proceedings of the Institution of Mechanical Engineers, Part G, Journal of Aerospace Engineering*, 217:123–142, 2003.
- [9] C.D. Lykins, S. Mall, and V. Jain. An evaluation of parameters for predicting fretting fatigue crack initiation. *International Journal of Fatigue*, 22(8):703–716, 2000. doi:[10.1016/S0142-1123\(00\)00036-0](https://doi.org/10.1016/S0142-1123(00)00036-0).
- [10] Y. Mutoh and J.Q. Xu. Fracture mechanics approach to fretting fatigue and problems to be solved. *Tribology International*, 36:99–107, 2003. doi:[10.1016/S0301-679X\(02\)00136-6](https://doi.org/10.1016/S0301-679X(02)00136-6).
- [11] N.S. Ottosen, R. Stenström, and M. Ristinmaa. Continuum approach to high-cycle fatigue modeling. *International Journal of Fatigue*, 30(6):996–1006, June 2008. doi:[10.1016/j.ijfatigue.2007.08.009](https://doi.org/10.1016/j.ijfatigue.2007.08.009).
- [12] R. Rabb. *Todennäköisyysteoriaan pohjautuva väsymisanalyysi*. BoD - Books on Demand, Helsinki, Finland, 2013.

- [13] C. Ruiz, P.H.B. Poddington, and K.C. Chen. An investigation of fatigue and fretting in a dovetail joint. *Experimental Mechanics*, 24:208–217, 1984.
- [14] D. Taylor. Geometrical effects in fatigue: a unifying theoretical model. *International Journal of Fatigue*, 21:413–420, 1999. doi:[10.1016/S0142-1123\(99\)00007-9](https://doi.org/10.1016/S0142-1123(99)00007-9).
- [15] A.A. Walvekar, B.D. Leonard, F. Sadeghi, B. Jalalahmadi, and N. Bolander. An experimental study and fatigue damage model for fretting fatigue. *Tribology International*, 79:183–196, 2014. doi:[10.1016/j.triboint.2014.06.006](https://doi.org/10.1016/j.triboint.2014.06.006).

Sami Holopainen, Reijo Kouhia
Tampere University of Technology,
Department of Mechanical Engineering and Industrial Systems
P.O. Box 589, FI-33101 Tampere
sami.holopainen@tut.fi, reijo.kouhia@tut.fi

Janne Juoksukangas and Arto Lehtovaara
Tampere University of Technology,
Department of Materials Science
P.O. Box 589, FI-33101 Tampere
janne.juoksukangas@tut.fi, arto.lehtovaara@tut.fi

Timo Saksala
Tampere University of Technology,
Department of Civil Engineering
P.O. Box 600, FI-33101 Tampere
timo.saksala@tut.fi